# Endothermic Formation of a Chemical Bond by Entropic Stabilization: Difluoronitroxide Radical in Solid Argon

**Eugenii Ya. Misochko,**[†] **Alexander V. Akimov,**[†] **Ilya U. Goldschleger,**[†]
**Alexander I. Boldyrev,**[‡] **and Charles A. Wight\*,[‡]**

*Contribution from the Institute for Chemical Physics Research, Russian Academy of Sciences,
142432 Chernogolovka, Moscow Region, Russia, and Department of Chemistry, University of Utah,
Salt Lake City, Utah 84112*

*Received June 25, 1998*

**Abstract:** Difluoronitroxide radical ($F_2NO$) has been formed in solid argon matrices by successive addition of two diffusing F atoms to NO. This radical exists in dynamic equilibrium with a van der Waals complex (F−FNO). Measurements of the equilibrium concentrations as a function of temperature show that the changes in enthalpy and the entropy associated with formation of the $F_2NO$ radical are $\Delta H = 1240 \pm 180$ J/mol and $\Delta S = 62 \pm 10$ J/(mol K). Because both these quantities are positive, the equilibrium favors $F_2NO$ only at elevated temperatures. This situation is a rare case in which formation of a chemical bond is stabilized only by an increase in the entropy of the system.

## Introduction

When an atom and a molecule come together in the gas phase to form a chemical bond between them, the system undergoes a significant change in the types of degrees of freedom. Because the product of such a reaction is a single molecule, three translational degrees of freedom are converted to vibrational modes. The density of translational states of gases is always higher than that for rotations and vibrations, so the reaction

$$A + BC \leftrightarrow ABC \tag{1}$$

always involves a reduction in entropy. Furthermore, the formation of the bond itself lowers the electronic energy of the system, so the change in enthalpy is also negative.

$$\Delta H < 0 \qquad \Delta S < 0 \tag{2}$$

If the reactants and products coexist in dynamic equilibrium, then the maximum concentration of ABC will occur at the lowest temperature; raising the temperature will invariably enhance the probability that the bond is broken.

In this paper, we report an unusual case in which the situation is exactly reversed. The changes in entropy and enthalpy associated with bond formation are both positive (i.e., bond formation is endothermic and endergonic). Nevertheless, the process is observable because the reaction takes place within the confines of a rare gas matrix and because the reactant consists of a van der Waals complex of the atom and molecule, rather than as two translationally free species.

We recently reported[1] that $F_2NO$ and F−FNO are formed in an argon matrix containing NO and $F_2$ when samples are photolyzed at 355 nm and subsequently annealed at 24 K for 100 min. The method takes advantage of the ability of F atoms to diffuse long distances through solid argon at temperatures

above 20 K (i.e., well below its melting point),[2,3] thereby forming unstable radicals and reaction intermediates that are isolated from photolytic precursor molecules.[3−7] A propitious combination of EPR and FTIR spectroscopic detection (carried out in separate experiments under similar conditions) allowed us to unambiguously identify the $F_2NO$ radical and to report its fundamental vibrational frequencies for the first time. In addition, the infrared experiments revealed the existence of an F−FNO complex that was observed to undergo reversible transformation to the $F_2NO$ radical in solid argon at cryogenic temperatures. Here, we report the details of that transformation,

$$[\text{F−FNO}] \underset{k_-}{\overset{k_+}{\rightleftharpoons}} F_2NO \tag{3}$$

in which formation of the second of the two N−F bonds is favored at elevated temperatures.

## Experimental Section

Samples of nitric oxide and fluorine were prepared in an argon matrix by vapor deposition of Ar:NO and Ar:$F_2$ mixtures onto a CsI salt window maintained at 16 K by a closed-cycle helium refrigerator. The gas mixtures are prepared in separate stainless steel manifolds and the two streams are mixed together as they exit the deposition tubes just prior to condensation on the cold window. The sample chamber is constructed of polished stainless steel and ultrahigh vacuum flanges. It is pumped by a 50 L/s turbomolecular pump; the base pressure of this apparatus is typically $5 \times 10^{-5}$ Pa.

Fluorine was obtained from Spectra Gases, Inc. as a mixture of 10% $F_2$ in argon and was used without further purification except as noted

† Russian Academy of Sciences.
‡ University of Utah.
(1) Misochko, E. Ya.; Akimov, A. V.; Goldschleger, I. U.; Wight, C. A. Infrared and EPR Spectra of the Difluoronitroxide Radical. *J. Am. Chem. Soc.* **1998,** *120,* 11520.

(2) Feld, J.; Kunti, H.; Apkarian, V. A. *J. Chem. Phys.* **1990,** *93,* 1009.
(3) Misochko, E. Ya.; Benderskii, V. A.; Goldschleger, A. U.; Akimov, A. V.; Benderskii, A. V.; Wight, C. A. *J. Chem. Phys.* **1997,** *106,* 3146.
(4) Misochko, E. Ya.; Benderskii, V. A.; Goldschleger, A. U.; Akimov, A. V. *Mendeleev Commun.* **1995,** *5,* 198.
(5) Goldschleger, A. U.; Misochko, E. Ya.; Akimov, A. V.; Goldschleger, I. U.; Benderskii, V. A. *Chem. Phys. Lett.* **1997,** *267,* 288.
(6) Benderskii, V. A.; Goldschleger, A. U.; Akimov, A. V.; Misochko, E. Ya.; Wight, C. A. *Mendeleev Commun.* **1995,** *6,* 203.
(7) Misochko, E. Ya.; Akimov, A. V.; Wight, C. A. *Chem. Phys. Lett.* **1998,** *293,* 547.

below. Nitric oxide was purchased from Matheson Gases and was purified by vacuum distillation prior to sample preparation. The argon diluent gas (99.999%) was also purchased from Spectra Gases.

The reagent mixtures were typically prepared at mole ratios of 6.7 $\times$ $10^{-4}$, so that deposition of equal volumes from the two manifolds produced samples that have nominal concentrations, Ar:NO:$F_2$ = 3000: 1:1. However, it was observed that some reaction of the fluorine invariably occurs in the manifold and deposition line, so that its actual concentration in the matrix is reduced by as much as 30−50% relative to the intended concentration. A portion of the stainless steel deposition line between the cold window and the gas-metering valve was immersed in liquid nitrogen during sample deposition to remove any impurities formed by reactions in the manifold.

Ultraviolet laser photolysis of the prepared matrixes was performed with use of the third harmonic of a Nd:YAG laser (Continuum model Surelight) at 355 nm. The laser entered the sample chamber through a fused silica window and impinged on the sample at an incident angle of 45°. The beam was expanded to an area of about 3.5 $cm^2$ at the sample to ensure uniform irradiation. The laser was operated at 10 pulses per second. Each laser pulse is nominally 7 ns in duration, and the average light intensity at the sample was 10 $mW/cm^2$ during photolysis.

The quantum yield for photodissociation of $F_2$ in solid argon[2] at 355 nm is 0.35−0.5. In a typical experiment, the sample was deposited and subsequently irradiated with 355 nm light (10 $mW/cm^2$ for 200 min at 16 K) to dissociate essentially all of the $F_2$ to F atoms. Then the sample was annealed at $T$ > 20 K to allow the F atoms to diffuse through the argon matrix and react with NO molecules. Infrared spectra were obtained at stages during the experiment by averaging 32 scans at 0.5 $cm^{-1}$ resolution with a Mattson model RS10000 FTIR spectrometer. The interferometer and detector are located on opposite sides of the sample chamber, which is equipped with two ZnSe windows to transmit the infrared beam. This arrangement allows transmission FTIR spectra to be obtained before, after, or during laser photolysis.

The EPR experiments were carried out in a similar manner. Details of the apparatus and techniques were described previously.[3] Samples were deposited onto a sapphire rod at 16 K and irradiated with 337 nm light (50 $mW/cm^2$ for 60 min at 16 K). They were then annealed at 24 K for 100 min to allow the F atoms to diffuse and react with NO.

## Results

**Infrared Spectra.** Illustrated in Figure 1 are FTIR spectra of an argon matrix containing $F_2$ and NO. The spectrum obtained immediately after deposition (trace a) shows bands due to NO, $(NO)_2$, FNO, and NOF. Exhaustive photolysis of the $F_2$ at 16 K produced very little change in the spectrum. However, annealing for 100 min at 26 K results in the formation of several product bands (trace b) that were identified as $FO_2$, $F_3NO$, and $F_2NO$. The last of these is a new species whose infrared bands were identified for the first time in a preliminary report of this work.[1] A key piece of evidence for identifying the $F_2NO$ radical was the observation of its EPR spectrum in experiments carried out under similar conditions (vide infra). Kinetic evidence[1] shows that this species is an intermediate in the sequential addition of F atoms to NO, forming FNO, $F_2NO$ and $F_3NO$ provided support for the assignment. Finally, the observed vibrational frequencies (1573, 813, 761, 705, and 553 $cm^{-1}$) are in good agreement with those calculated by ab initio quantum theory (vide infra).

Also observed in the infrared spectra of the reaction products are two doublets at 1800 (1884) and 719 (714) $cm^{-1}$. Ordinarily, these bands would not have attracted much attention. However, we observed that by changing the temperature of the sample in the interval 17−30 K, this product can be reversibly converted to the $F_2NO$ radical and back again (see trace d of Figure 1). The reversible temperature conversation of $F_2NO$ means that this new species must be composed from the same atoms. This
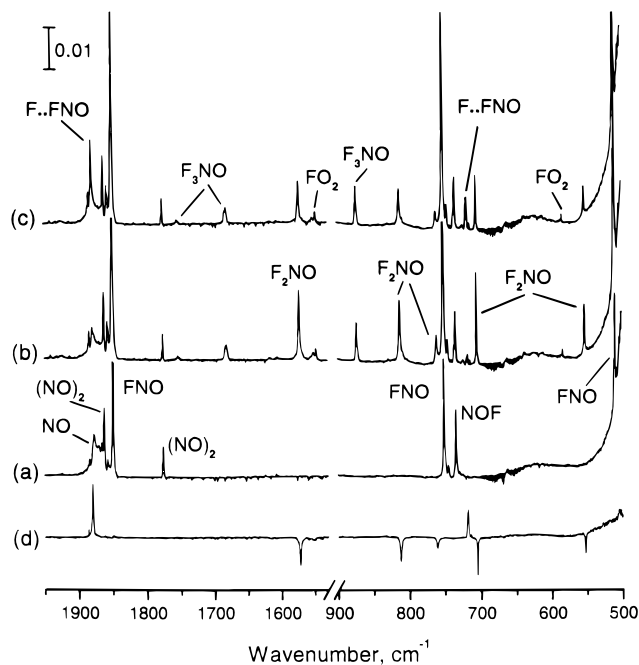


**Figure 1.** Infrared spectra of a sample (Ar:NO:$F_2$ = 2000:1:1) after deposition at 16 K (trace a), after exhaustive photolysis at 16 K and subsequent annealing for 100 min at 26 K (trace b), and after subsequent annealing for 1000 min at 20 K (trace c). Trace d shows difference spectra of traces c and b. All spectra were recorded at 16 K.
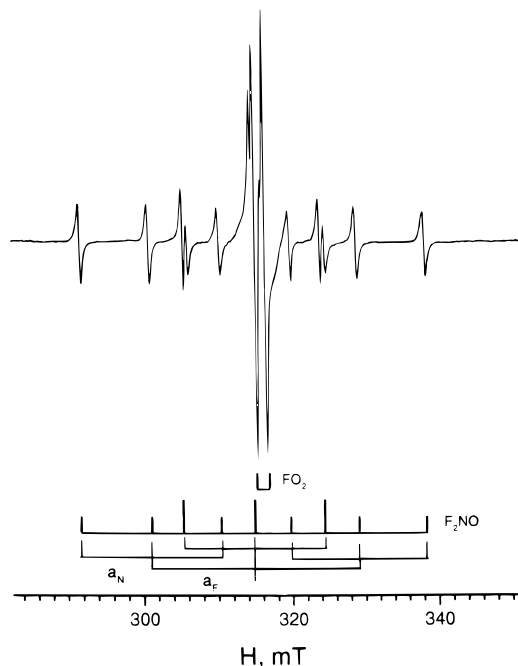


**Figure 2.** EPR spectrum of the $F_2NO$ radical in solid argon at 30 K. The stick spectrum shows the characteristic triplet of triplets pattern, as well as overlapping bands due to $FO_2$ impurity radicals.

observation, coupled with the fact that the pair of doublets lie close to the frequencies of FNO and NOF, led us to assign the doublets to the van der Waals complex F−FNO. A summary of the infrared bands observed in this study is presented in Table 1.

**EPR Spectra.** Figure 2 illustrates the EPR spectra of a sample following low-temperature UV laser photolysis followed by annealing at 24 K. This spectrum, which was obtained at 30 K, consists of nine narrow lines (a triplet of triplets) that are characteristic of a radical that contains two equivalent fluorine
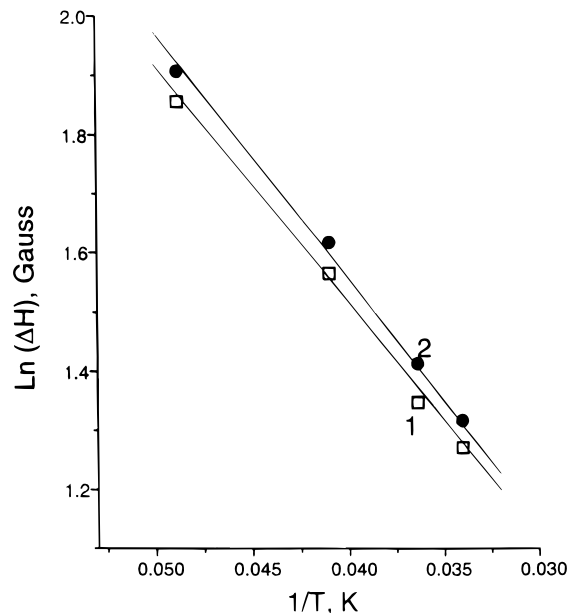
**Table 1.** Frequencies, Assignments, and Integrated Absorption Coefficients for Reactants and Products in Photolyzed Solid Mixtures of Ar:F₂:NO

| freq, cm⁻¹ | assignment and integrated absorption cross sections (km/mol) | | | | |
|---|---|---|---|---|---|
| | NO | FNO | (FNO···F) | F₂NO | F₃NO[a] |
| 1884 | | (FON)[b] | | | |
| 1880 (1884) | | | $\nu_1$ (FNO) | | |
| 1877.4 | isolated NO,[b] | | | | |
| 1871.6 | 35 ± 5 (30 ± 5)[c] | | | | |
| 1866.5 | | | | | |
| 1863.1 | (NO)₂[d] | | | | |
| 1862.6 | NO−F₂ | | | | |
| 1849.6 (1851) | | $\nu_1$, 114 ± 25 (125.0)[e] | | | |
| 1776.1 | (NO)₂[d] | | | | |
| 1754.2 | | | | | $2\nu_4$, 120 ± 30 |
| 1681.4 | | | | | $\nu_1$ |
| 1572.7 | | | | $\nu_1$, 77 ± 20 | |
| 905 | | | | | |
| 873.4 | | | | | $\nu_4$, 370 ± 80 |
| 813 (808) | | | | $\nu_5$, 65 ± 15 | |
| 761 | | | | $\nu_2$ | |
| 751 (746) | | $\nu_2$, 95 ± 20 (92.5)[e] | | | |
| 740.5 | | | | | $\nu_2$ |
| 734.5 | | (FON)[b] | | | |
| 719 (714) | | | $\nu_2$, (FNO) 62 ± 15 | | |
| 705 (703) | | | | $\nu_3$, 48 ± 10 | |
| 552.7 | | | | $\nu_6$ | |
| 529 | | | | | $\nu_3$ |
| 509.8 | | $\nu_3$ | | | |

[a] Assigned in ref 13. [b] Assigned in ref 14. [c] Gas-phase value from ref 15. [d] Assigned in ref 16. [e] *Ab initio* calculation from ref 17.

nuclei (hyperfine constant $a_F = 143$ G) and one nitrogen nucleus ($a_N = 93$ G), and corresponds to the F₂NO radical.[8,9,10,11] At the center of the spectrum, the spectral lines are overlapped by lines due to the FO₂ radical,[12] which is formed by addition of diffusing F atoms to O₂ impurity molecules. The outer lines of the F₂NO radical are well-resolved and have strongly temperature-dependent line widths. In Figure 3, the measured half-widths of two outer lines are presented as a function of the sample temperature. The anisotropy of the fluorine hyperfine constants is very large ($\Delta a_F \sim 10$ mT), as reported in our prior paper,[1] and the temperature dependence of the line width is caused by incomplete averaging of the anisotropy due to hindered molecular rotation in the matrix.

**Kinetics of F₂NO Formation.** Figure 4 shows the relative concentrations of NO, FNO, F₂NO, F−FNO, and F₃NO during the annealing period at 24 K after 355 nm laser photolysis at 16 K. By comparing the relative intensities of the bands and using a mass balance equation based on the assumption that all these species contain only one NO functional group, it was possible to determine integrated absorption coefficients for the various bands. These values are listed in Table 1, together with some gas-phase values that were taken from the literature.[13−17] Note that under the conditions of Figure 4, the kinetic behavior of F−FNO is that of a precursor to F₂NO, and that near the end of the annealing period the concentration of F₂NO is much greater than that of F−FNO.

(8) Vanderkooi, N.; Mackenzie, J. S.; Fox, W. B. *J. Fluorine Chem.* **1976**, *7*, 415.
(9) Nishikida, K.; Williams, F. *J. Am. Chem. Soc.* **1975**, *97*, 7168.
(10) Morton, J. R.; Preston, K. F. *J. Chem. Phys.* **1980**, *73*, 4914.
(11) Morton, J. R.; Preston, K. F. *J. Chem. Phys.* **1981**, *75*, 1126.
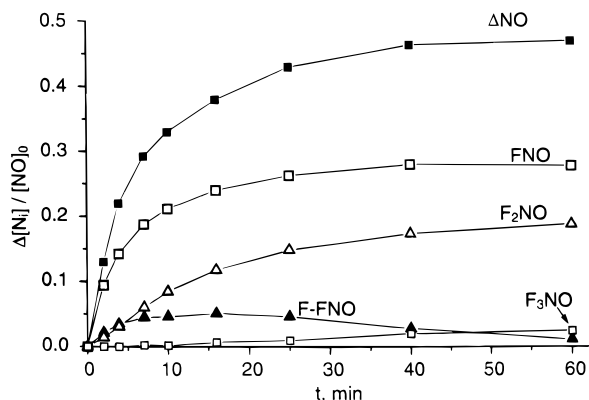(12) Adrian, F. J. *J. Chem. Phys.* **1967**, *46*, 1543.
(13) Smardzewski, R. R.; Fox, W. B. *J. Chem. Phys.* **1974**, *60*, 2193.
(14) Smardzewski, R. R.; Fox, W. B. *J. Chem. Phys.* **1974**, *60*, 2104.
(15) Michels, H. H. *J. Quantum Spectrosc. Radiat. Tranfer.* **1971**, *11*, 1735.
(16) Guillory, W. A.; Hunter, C. E. *J. Chem. Phys.* **1969**, *50*, 3516.
(17) Ford, T. A.; Agnew, S. F.; Swanson, B. I. *J. Mol. Struct.* **1993**, *297*, 255.



**Figure 3.** Plot of the natural logarithm of measured EPR line widths of F₂NO as a function of inverse absolute temperature: 1, low-field line ($m_F = -1$, $m_N = -1$); 2, − high-field line ($m_F = 1$, $m_N = 1$).

The kinetic behavior observed illustrated in Figure 4 is consistent with an overall reaction scheme

$$F + NO \rightarrow FNO \qquad (4)$$

$$F + FNO \rightarrow F-FNO \qquad (5)$$

$$F-FNO \rightarrow F_2NO \qquad (6)$$

$$F + F_2NO \rightarrow F_3NO \qquad (7)$$

After about 100 min of annealing at 24 K, the concentrations of all observed species reach their limiting values, and no additional reactions are observed. This is due to the recombina-

**Figure 4.** Kinetics of consumption of reactant molecules ($\Delta$NO) and accumulation of reaction products during 24 K annealing of a sample (Ar:NO:$F_2$ = 2000:1:1) that was exhaustively photolyzed at 16 K. All concentrations are given relative to the initial concentration of NO molecules in the sample.

**Table 2.** Relative Concentrations of NO and Fluorinated Products in Ar:$F_2$:NO = 8000:3:1 after Cycles of Photolysis and Annealing

|  | NO[a] | FNO[b] | $F_2NO$[b] | $F_3NO$[b] |
|---|---|---|---|---|
| after 1st photolysis and 90 min annealing at 26 K | 0.32 | 0.22 | 0.38 | 0.08 |
| after 2nd photolysis and annealing | 0.15 | 0.21 | 0.48 | 0.16 |
| after 3rd photolysis and annealing | 0.10 | 0.19 | 0.46 | 0.25 |
| after 4th photolysis and annealing | 0.04 | 0.16 | 0.46 | 0.34 |

[a] Fraction of initial NO concentration remaining. [b] Concentration relative to initial concentratino of NO.

tion of the diffusing F atoms with the various species, including recombination with other F atoms to regenerate the fluorine photolytic precursor,

$$F + F \rightarrow F_2 \tag{8}$$

Some samples were subjected to additional cycles of 16 K photolysis and annealing at $T > 20$ K. In these cases, it was observed that additional F atoms were made available for reaction, and there was a greater extent of conversion of NO and FNO to their more fluorinated reaction products. For example, the relative concentrations of fluorinated products that formed in four subsequent cycles of photolysis and annealing are shown in Table 2. It can be seen that under these conditions more than 96% of the NO can be converted to fluorinated products, including a nearly 50% yield of $F_2NO$ radicals and 35% yield of $F_3NO$ molecules. The relative concentration of $F_3NO$ is increased in each cycle, consistent with the reaction scheme (4–7).

The sample was then cooled to 16 K and photolyzed for a period of only 5 min. This brief photolysis resulted in the complete destruction of $F_2NO$ and the appearance of the van der Waals complex F–FNO in its place. Heating of the sample to 26 K leads to a prompt recovery of the $F_2NO$ bands and disappearance of the F–FNO bands. Similar behavior was observed for the EPR spectra of radicals in photolyzed and annealed Ar/$F_2$/NO samples. Short-time photolysis at 16 K results in complete disappearance of EPR spectra of the $F_2NO$ radical. Subsequent annealing of the sample to 26 K causes the EPR spectrum of $F_2NO$ to be completely recovered. No other radical products are observed. It is worth mentioning that EPR spectra of F–FNO complexes and F atoms in an argon matrix are not detected due to severe anisotropic broadening of the bands.[1]

These observations demonstrate unambiguously that the $F_2NO$ radical is dissociated by 355 nm light to the open-shall van der
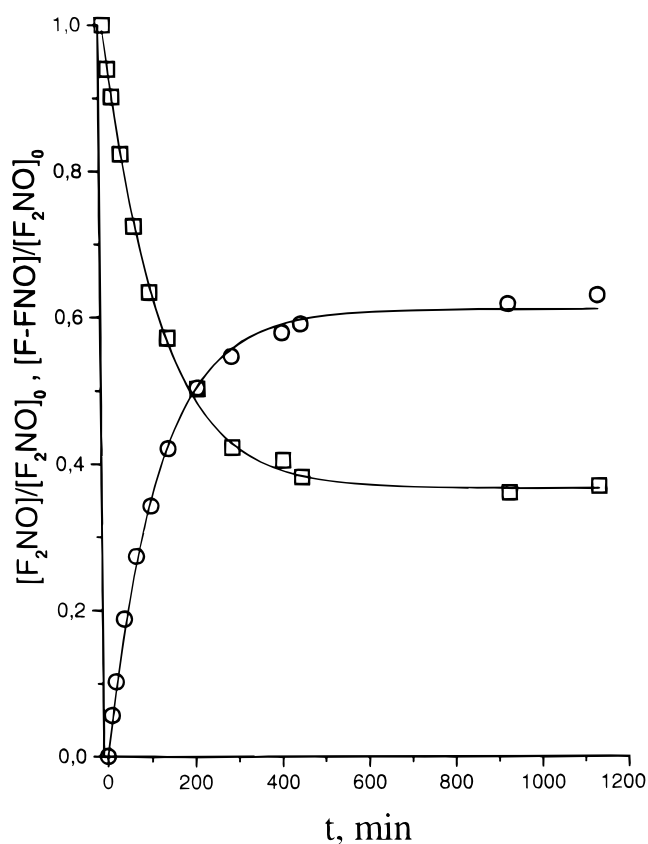


**Figure 5.** Kinetic plot of the dissociation reaction of $F_2NO$ (open squares) to the van der Waals complex F–FNO (open circles) following a lowering of the sample temperature from 30 to 20 K. The curves are single-exponential fits to the data, rate constant $k = 1.4 \times 10^{-4}$ s$^{-1}$.

Waals complex F–FNO in solid argon. However, the complex F–FNO is unstable at 26 K with respect to thermally activated conversion back to the $F_2NO$ radical. The equilibrium constant of reaction 3 at 26 K is

$$K_{26K} = \frac{[F_2NO]_{26K}}{[F - FNO]_{26K}} = 6.1 \pm 1.2 \tag{9}$$

**Thermal Interconversion of F–FNO and $F_2NO$.** The thermally activated conversion of F–FNO to $F_2NO$ in the dark following photolysis initially led us to the conclusion that formation of the second N–F bond in the radical is exothermic. Therefore, it took us by surprise that when the sample was cooled to lower temperatures, the $F_2NO$ began to disappear and was replaced by a corresponding growth of the infrared bands corresponding to the F–FNO complex, as illustrated in Figure 1 (traces c and d). The kinetics of this conversion at 20 K (see Figure 5) are exponential with a characteristic rate constant of $1.4 \times 10^{-4}$ s$^{-1}$. The relative concentration of product and reactant at equilibrium is

$$K_{20K} = \frac{[F_2NO]_{20K}}{[F - FNO]_{20K}} = 0.60 \pm 0.12 \tag{10}$$

Subsequent heating of the sample to 26 K resulted in complete recovery of the $F_2NO$ radical in less than 5 min, as was described in the previous section for the dark reaction following photolysis.

Because $K_{20} < K_{26}$ the N–F bond formation in reaction 3 must be endothermic! To determine the enthalpy of reaction 3, several measurements of the equilibrium concentrations of $F_2$-
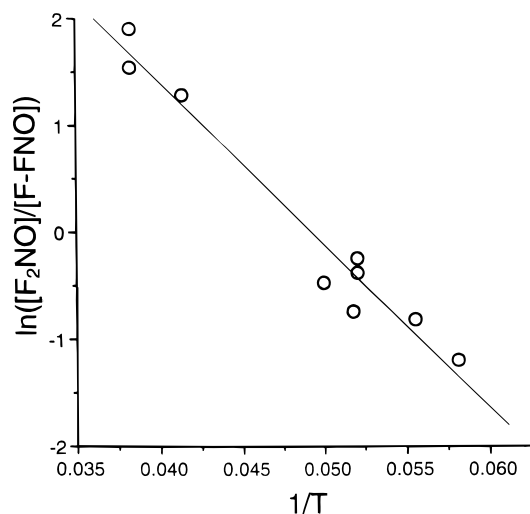
**Figure 6.** Logarithmic plot of the equilibrium constant for reaction 3 as a function of inverse absolute temperature.

**Table 3.** Structure, Energy, and Vibrational Frequencies of FNO

| property | QCISD/ cc-pvdz | QCISD(T)/ cc-pvdz | QCISD/ 6-311+G* | experiment |
|---|---|---|---|---|
| $R$(N−O), nm | 0.1148 | 0.1151 | 0.1138 | 0.1136 |
| $R$(N−F), nm | 0.1496 | 0.1524 | 0.1501 | 0.1512 |
| ∠FNO, deg | 110.04 | 110.23 | 110.01 | 110.08 |
| $E_{tot}$, hartrees | −229.187727 | −229.206242 | −229.280062 | |
| $\omega_1$(a′), cm$^{-1}$ | 1889 | 1861 | 1901 | 1843.5 |
| $\omega_2$(a′), cm$^{-1}$ | 810 | 783 | 789 | 765.8 |
| $\omega_3$(a′), cm$^{-1}$ | 546 | 513 | 525 | 515.9 |

NO and F−FNO as a function of temperature were made. From a linear least-squares fit of these data, which are plotted in Figure 6, the changes in enthalpy and entropy for the interconversion, reaction 3, were determined to be

$$\Delta H = 1240 \pm 180 \text{ J/mol}$$

$$\Delta S = 62 \pm 10 \text{ J/mol K}$$

(11)

The uncertainties are limited by the accuracy of the relative concentration measurements rather than the linear fits to the experimental data. This result shows that formation of the second N−F bond in the F$_2$NO radical is endothermic. Furthermore, the reaction is accompanied by a significant increase in entropy, more than six times the universal gas constant, $R$.

**Theoretical Calculations**

We carried out several quantum chemical calculations to provide support for our assignments of the infrared spectra and to provide additional insight to the energetics of bond formation between F and FNO.

The first series of calculations was performed for FNO. This was done in part to determine the reliability of the different computational methods used. These results are presented in Table 3. The QCISD method, when used with the larger 6-311++G** basis set, yields structural parameters that are in nearly perfect agreement with the experimental values. The calculated harmonic vibrational frequencies differ by only 3% from the experimentally observed fundamental frequencies.

The same methods were then used to calculate the properties of F$_2$-NO radical, and these results are presented in Table 4. All three combinations of method and basis set gave similar bond lengths and bond angles. The agreement with the frequencies of the five infrared bands assigned to F$_2$NO in this work is good. At the highest level of theory (QCISD/6-311++G**), the maximum relative error is 17% and the root-mean-square relative error is only 8%. Therefore, the compu-

**Table 4.** Structure, Energy, and Vibrational Frequencies of F$_2$NO

| property | QCISD/ cc-pvdz | QCISD(T)/ cc-pvdz | QCISD/ 6-311++G** | experiment (ref 1) |
|---|---|---|---|---|
| $R$(N−O), nm | 0.1183 | 0.1176 | 0.1179 | |
| $R$(N−F), nm | 0.1435 | 0.1475 | 0.1423 | |
| ∠FNO, deg | 116.88 | 117.11 | 116.74 | |
| ∠FNF, deg | 102.11 | 101.82 | 102.24 | |
| $E_{tot}$, hartrees | −328.708229 | −328.730038 | −328.845002 | |
| $\omega_1$(a′), cm$^{-1}$ | 1580 | 1659 | 1557 | 1573 |
| $\omega_2$(a′), cm$^{-1}$ | 747 | 710 | 761 | 761 |
| $\omega_3$(a′), cm$^{-1}$ | 598 | 533 | 613 | 705 |
| $\omega_4$(a″), cm$^{-1}$ | 422 | 354 | 438 | |
| $\omega_5$(a″), cm$^{-1}$ | 863 | 806 | 877 | 813 |
| $\omega_6$(a″), cm$^{-1}$ | 450 | 393 | 472 | 553 |

**Table 5.** Calculated N−F Bond Dissociation Energies of F$_2$NO

| method/basis set[a] | BDE,[b] kJ/mol | BDE+ZPE,[c] kJ/mol | total energy (au) |
|---|---|---|---|
| CCSD/cc-pvdz | −15.52 | −23.97 | −328.703 403 |
| CCSD(T)/cc-pvdz | −12.38 | −20.17 | −328.726 615 |
| CCSD/aug-cc-pvdz | −0.25 | −8.70 | −328.788 109 |
| CCSD(T)/aug-cc-pvdz | 5.15 | −2.64 | −328.817 714 |
| QCISD/6-311++G** | 12.64 | 3.68 | −328.845 002 |
| CCSD/cc-pvtz | 9.87 | 1.42 | −329.016 388 |
| CCSD(T)/cc-pvtz | 17.24 | 9.46 | −329.055 703 |
| G1 | 15.48 | 6.53 | −329.105 201 |
| G2 | 19.12 | 10.17 | −329.107 558 |

[a] All energy calculations were performed at the optimal QCISD/6-311++/G** geometry. [b] Classical value, $D_e$, not including zero-point energy corrections. [c] Zero-point energy corrections were calculated at the QCISD/6-311++/G** level of theory.

tational results strongly support the assignment of these five bands to the F$_2$NO radical. The experimentally observed frequencies were reported for the first time in a preliminary account of this work.[1]

We next turned to calculating the strength of the NF bond in the F$_2$NO radical. The fact that the experiments show reversible interconversion of F−FNO and F$_2$NO indicate that this bond is exceptionally weak, or perhaps metastable; the calculations bear this out. Table 5 lists the bond dissociation energies calculated by using several different combinations of methods and basis set in order of increasing accuracy. At the highest level of theory, the results indicate that gas-phase F$_2$NO is stable with respect to dissociation of one N−F bond, but only by about 10 kJ/mol.

**Discussion**

The measurements of equilibrium relative concentrations of F−FNO and F$_2$NO as a function of temperature clearly show that low temperatures favor dissociation of the N−F bond, and the highest concentrations of F$_2$NO are observed at elevated temperatures. This result shows that formation of the second N−F bond in the F$_2$NO radical is endothermic by 1240 ± 180 J/mol and that the reaction is accompanied by an increase in entropy of 62 ± 10 J/(mol K).

A direct comparison of these values with *ab initio* quantum calculations is not possible because the calculations are strictly for gas-phase species. At the highest level of theory, the calculations predict that in the gas phase, N−F bond formation is very slightly exothermic (bond dissociation energy of 10 kJ/mol). In solid argon, the initial state is a van der Waals complex, F−FNO, not the free species F + FNO. Therefore, the binding energy of the complex and differential solvent effects must be considered to make a direct comparison between theory and experiment. We attempted to calculate the energy of the F−FNO complex, but were unable to locate the equilibrium geometry due to difficulty in SCF and QCI convergences. Future experiments in other matrices (krypton and xenon) will be performed to clarify the influence of solid environment on the

reaction exothermicity. However, for purposes of qualitative comparison, the *ab initio* calculations show that the experimental result presented here is a reasonable one.

What makes this system particularly interesting is the observation that the entropy of the $F_2NO$ radical is greater than that of the van der Waals complex F−FNO. An important clue for why this might be so comes from the EPR data. In our preliminary report,[1] we noted that the F−FNO complex was not observed at all by EPR because the anisotropy of the **g** tensor and the hyperfine constants causes the lines to be severely broadened. For this reason, neither F atoms nor any complexes of F with closed-shell molecules have ever been observed in rare gas matrices by EPR. The fact that the isotropic EPR spectrum of the $F_2NO$ radical is observed at $T > 20$ K provides strong evidence that the radical undergoes hindered rotational motion in solid argon on a time scale that is comparable with the characteristic time of the EPR measurement. We have estimated the rotational correlation time from the spectral line widths in the limit that the radicals undergo rapid incoherent rotation to be[18,19]

$$\tau_c \sim 18 H_0 \Delta H / \omega_0 \Delta a_F^2 = 10^{-9}\ \text{s} \quad (12)$$

at 25 K. The temperature dependence of the line widths allows us to estimate the barrier to hindered rotation from the slope of the plot shown in Figure 3. The result is an estimated barrier $V_0 \sim 35$ cm$^{-1}$.

The rotational entropy of $F_2NO$ can be estimated in two limits: a librator (rotational harmonic oscillator) or a free rotor. The actual situation lies somewhere between these limits. For the free rotor, we have calculated the rotational constants and characteristic temperatures

$$A = 0.38\ \text{cm}^{-1} \quad T_A = 0.54\ \text{K}$$

$$B = 0.33\ \text{cm}^{-1} \quad T_B = 0.47\ \text{K}$$

$$C = 0.18\ \text{cm}^{-1} \quad T_C = 0.26\ \text{K} \quad (13)$$

from the moments of inertia of $F_2NO$ obtained in the ab initio calculations. Note that the corresponding rotational frequencies ($\sim 10^{10}$ s$^{-1}$) are only 1 order of magnitude greater than the observed hindered rotational correlation frequency ($\sim \tau_c^{-1}$) at 25 K. The free rotational partition function in the classical limit ($T \gg T_A$) is

$$Z_{\text{rot}} = \frac{T^{3/2}}{2(T_A T_B T_C)^{1/2}} \quad (14)$$

and the rotational entropy is

$$S_{\text{rot}} = \frac{\text{d}(RT \ln Z_{\text{rot}})}{\text{d}T} = \frac{3}{2}R + R \ln Z_{\text{rot}} \quad (15)$$

Over the experimental range of temperatures (17−26 K) this function spans the range 6.4−7.1 $R$.

For the other limit, that of a rotational harmonic oscillator, we can estimate the characteristic frequency of each of the three librational oscillators from the barrier height and the corresponding rotational constant

$$\tilde{\nu}_B \approx n(V_0 B)^{1/2} = n(0.695 \cdot V_0 T_B)^{1/2} = 13\ \text{cm}^{-1} \quad (16)$$

where we have estimated $n = 4$ to be the number of equivalent configurations of $F_2NO$ in an argon lattice site. The librational entropy is

$$S_{\text{lib}} = \sum_i R\left[\frac{x_i}{e^{x_i} - 1} - \ln(1 - e^{-x_i})\right] \quad (17)$$

where

$$x_i = hc\tilde{\nu}_i/kT$$

To this must be added a term to account for the configurational entropy

$$S_{\text{conf}} = R \ln n = 1.4R \quad (18)$$

The entropy in this limit spans the range 4.3−5.5 $R$ over the experimental range of temperatures.

If we assume that the van der Waals complex F−FNO has a large barrier to rotation ($>100$ cm$^{-1}$) then its rotational entropy will be negligible at $T < 30$ K, and the measured $\Delta S = 7.5R$ for the reaction is therefore quite reasonable in magnitude.

## Conclusions

We have detected and characterized the $F_2NO$ radical and a van der Waals complex F−FNO in a solid argon matrix. The two species undergo reversible interconversion at temperatures in the range 17−30 K. Measurements of the equilibrium concentrations as a function of temperature show that formation of $F_2NO$ in this reaction is endothermic and involves a substantial increase in entropy. The structure and weak N−F bond energy of $F_2NO$ has been verified by *ab initio* quantum chemical calculations.

This rare case of entropic stabilization of a chemical bond is realized only as a consequence of two effects of the solid-state environment. First, the reactant, F−FNO, is stabilized at low temperature as a van der Waals complex that does not have free translational or rotational motion, as it would in the gas phase. Second, the entropy of the product, $F_2NO$, is greatly enhanced by its ability to undergo rapid hindered rotation in the argon matrix. Because of this, the radical can occupy a relatively large density of states at $T > 20$ K, thereby reducing the rate of N−F bond dissociation relative to the bond formation rate.

JA982222R

(18) Freed, J. H.; Fraenkel, J. K. *J. Chem. Phys.* **1963**, *39*, 326.
(19) Fraenkel, J. K. *J. Phys. Chem.* **1967**, *71*, 139.